Iterative Solution of the Eigenvalue Problem for a Dielectric Waveguide

Albert T. Galick, Thomas Kerkhoven, and Umberto Ravaioli, *Member, IEEE*

Abstract—**We present a numerical approach to the simulation of dielectric waveguides that is free of spurious modes and is based on the solution of an eigenvalue problem for the two transverse components of the magnetic field. We introduce a new discretization which has several computational advantages. In particular, by careful design of the discretization procedure we obtain systems of equations for the two components which are equivalent in the sense that a rotation over 90° corresponds to a suitable permutation of indices. The eigenvalue problem is solved iteratively by using an adapted version of the Chebyshev–Arnoldi algorithm. This approach takes full advantage of the sparsity of the matrix and circumvents the large memory requirements and the large computational complexity associated with dense methods. This allows us to employ meshes that are sufficiently fine to resolve higher modes without large discretization errors.**

I. Introduction

DIELECTRIC channel waveguides are widely used for integrated circuit applications, from the microwave to the optical frequency range. For an accurate analysis of general waveguide structures of practical interest, numerical solutions are necessary. As pointed out in [1], [2], reliable simulation software should employ formulations which are free of spurious modes, for instance by solving directly the vector Helmholtz equation in terms of the transverse magnetic field components H_x and H_y. Discretization of this vector equation leads to an eigenvalue problem which implicitly includes the zero divergence relation for the magnetic field, with consequent elimination of spurious modes. This requires dealing with a larger, nonsymmetric, discretized matrix. The size is particularly problematic if the solution is obtained with standard dense eigenvalue solvers, which can only handle a relatively small number of mesh points, even on the largest supercomputers available.

Manuscript received July 25, 1991; revised November 5, 1991. This work was supported by the Office of Naval Research grant SDI-IST N00014-90-J-1270, the Department of Energy grant DE-FG02-85ER25001, and the National Science Foundation grants NSF CCR 87-17942 and NSF ECD 89-43166.

A. T. Galick is with the Center for Supercomputing Research and Development, University of Illinois at Urbana-Champaign, Urbana, IL 61801-2932.

T. Kerkhoven is with the Department of Computer Science and Department of Electrical and Computer Engineering, University of Illinois at Urbana-Champaign, Urbana, IL 61801-2932.

U. Ravaioli is with the Beckman Institute, Coordinated Science Laboratory, and Department of Electrical and Computer Engineering, University of Illinois at Urbana-Champaign, Urbana, IL 61801-2932.

IEEE Log Number 9106036.

In this paper we solve eigenvalue problems for the dielectric waveguide with an efficient implementation of the iterative Chebyshev–Arnoldi algorithm. Our approach has manageable memory requirements because it allows the matrix of the discretized problem to be stored in sparse form. Moreover, in this approach we impose the condition that the modes should be confined to the waveguide to select in advance a region in the complex plane where the eigenvalues should lie. This limits the number of eigenvalue/eigenvector pairs that are computed and, therefore, the computational complexity. Consequently, we can employ extensive nonuniform meshes with many grid points on which the discretization error can be controlled. As part of the project we developed a novel discretization scheme for the vector Helmholtz problem, where we obtain systems of equations for the two components which are equivalent in the sense that a rotation over 90° corresponds to a suitable permutation of indices.

II. Discretization Approach

We employ a 5-point finite-difference formula based on a box-integration method [3] depicted in Fig. 1. The cardinal points North (N), West (W), South (S), and East (E) are used as references around the center point (P). The mesh widths connecting P to the neighboring points are indicated by n, w, s, and e. The boxes Ω_i in Fig. 1 are delimited by the mesh lines n, w, s, and e and by their perpendicular bisectors. The dielectric permittivity inside each box Ω_i is assumed to be a constant ϵ_i.

We assume a wave dependence of $e^{i(\omega t - \beta z)}$ for the electromagnetic field. To ensure that spurious modes will not be present in the solution [1], [4], the H_z component is determined by

$$\nabla \cdot \boldsymbol{H} = \partial_x H_x + \partial_y H_y - i\beta H_z = 0. \tag{1}$$

Here and throughout the paper we use the shorthand notation $\partial_x = \partial/\partial_x$ and $\partial_{xx} = \partial^2/\partial_x^2$. We integrate the Helmholtz equations for H_x and H_y over each box Ω_i separately, using

$$\oint_{\partial\Omega_i} \nabla_t H_\alpha \cdot \boldsymbol{n}\, ds + (\omega^2 \mu \epsilon_i - \beta^2) \int_{\Omega_i} H_\alpha\, dA = 0, \tag{2}$$

where $\alpha = x$ or y, $\nabla_t = (\partial_x, \partial_y)$, $\partial\Omega_i$ is the boundary of Ω_i, and $\boldsymbol{n}$ is the unit outward normal of $\partial\Omega_i$. The first term

represents the fluxes through the boundary of the box Ω_i. We use $\partial_x H_y - \partial_y H_x = i\omega\epsilon E_z$ and Eq. (1) to restate the continuity of the axial field components E_z and H_z across an interface [5] in terms of the transverse magnetic field components:

$$(\partial_x H_y - \partial_y H_x)_i/\epsilon_i = (\partial_x H_y - \partial_y H_x)_j/\epsilon_j \tag{3}$$

$$(\partial_x H_x + \partial_y H_y)_i = (\partial_x H_x + \partial_y H_y)_j. \tag{4}$$

The box-integration and interface matching equations for H_x at P from (2), (3), and (4) are assembled into the matrix equation

$$\mathbf{0} = \left[\begin{array}{cccccccc} 1 & -1 & 0 & 0 & 0 & 0 & 0 & 0 \\ 0 & 0 & -1 & -1 & 0 & 0 & 0 & 0 \\ 0 & 0 & 0 & 0 & -1 & 1 & 0 & 0 \\ 0 & 0 & 0 & 0 & 0 & 0 & 1 & 1 \\ \hline & & & & \mathbf{0} & & & \\ \hline & & & & \mathbf{0} & & & \end{array}\right] \left[\begin{array}{c} \int_{1N} \partial_y H_x\, dx \\ \int_{1W} \partial_x H_x\, dy \\ \int_{2W} \partial_y H_x\, dy \\ \int_{2S} \partial_y H_x\, dx \\ \int_{3S} \partial_y H_x\, dx \\ \int_{3E} \partial_x H_x\, dy \\ \int_{4E} \partial_x H_x\, dy \\ \int_{4N} \partial_y H_x\, dx \end{array}\right] + \left[\begin{array}{c} 0 \\ 0 \\ 0 \\ 0 \\ \hline \left(\frac{1}{\epsilon_1} - \frac{1}{\epsilon_2}\right) \int_{1S} \partial_x H_y\, dx \\ \left(\frac{1}{\epsilon_4} - \frac{1}{\epsilon_3}\right) \int_{3N} \partial_x H_y\, dx \\ \hline 0 \\ 0 \end{array}\right]$$

$$+ \left[\begin{array}{c} (\omega^2\mu\epsilon_1 - \beta^2) \int_1 H_x\, da \\ (\omega^2\mu\epsilon_2 - \beta^2) \int_2 H_x\, da \\ (\omega^2\mu\epsilon_3 - \beta^2) \int_3 H_x\, da \\ (\omega^2\mu\epsilon_4 - \beta^2) \int_4 H_x\, da \\ \hline 0 \\ 0 \\ \hline 0 \\ 0 \end{array}\right] + \left[\begin{array}{cccccccc} 0 & 0 & 0 & 1 & -1 & 0 & 0 & 0 \\ 1 & 0 & 0 & 0 & 0 & 1 & 0 & 0 \\ 0 & -1 & 0 & 0 & 0 & 0 & 1 & 0 \\ 0 & 0 & -1 & 0 & 0 & 0 & 0 & -1 \\ \hline & & & & \frac{-1}{\epsilon_1} & \frac{1}{\epsilon_2} & 0 & 0 \\ & & & \mathbf{0} & & & & \\ & & & & 0 & 0 & \frac{1}{\epsilon_3} & \frac{-1}{\epsilon_4} \\ \hline 1 & -1 & 0 & 0 & & & & \\ & & & & & \mathbf{0} & & \\ 0 & 0 & -1 & 1 & & & & \end{array}\right] \left[\begin{array}{c} \int_{2E} \partial_x H_x\, dy \\ \int_{3W} \partial_x H_x\, dy \\ \int_{4W} \partial_x H_x\, dy \\ \int_{1E} \partial_x H_x\, dy \\ \hline \int_{1S} \partial_y H_x\, dx \\ \int_{2N} \partial_y H_x\, dx \\ \int_{3N} \partial_y H_x\, dx \\ \int_{4S} \partial_y H_x\, dx \end{array}\right] \tag{5}$$

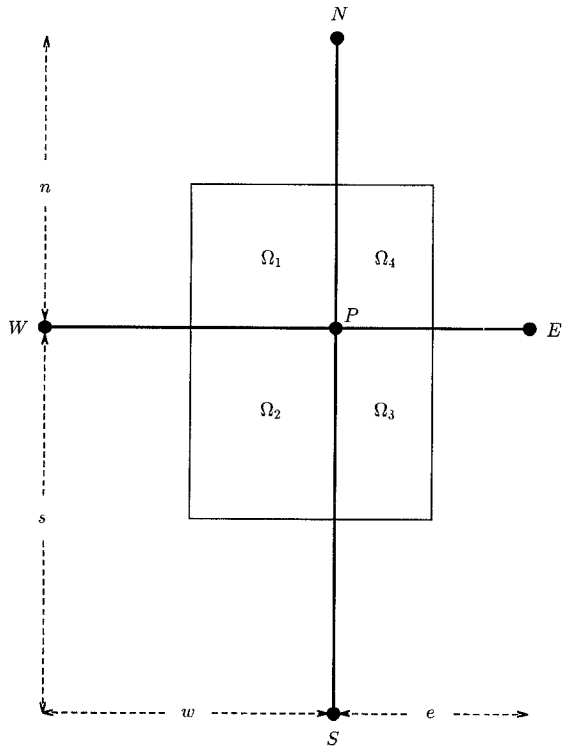

Fig. 1. The box integration scheme.

with 4 terms involving exterior fluxes, coupling terms, box integrals, and interior fluxes. If the 8×8 matrix in the last term is singular, i.e., if $\epsilon_1^{-1}\epsilon_3^{-1} - \epsilon_2^{-1}\epsilon_4^{-1} = 0$, then all interior fluxes are eliminated by taking an appropriate linear combination of the rows in (5). Otherwise, the interior fluxes that cannot be eliminated are approximated by one-sided differences. The exterior fluxes of the union of the Ω_i are approximated by centered differences as in the standard box-integration scheme. The choice of coefficients:

$$\left(\sqrt{\frac{\epsilon_2}{\epsilon_1}}, \sqrt{\frac{\epsilon_1}{\epsilon_2}}, \sqrt{\frac{\epsilon_4}{\epsilon_3}}, \sqrt{\frac{\epsilon_3}{\epsilon_4}}, -\sqrt{\epsilon_1\epsilon_2}, -\sqrt{\epsilon_3\epsilon_4}, -\frac{1}{2}\left(\sqrt{\frac{\epsilon_1}{\epsilon_2}} + \sqrt{\frac{\epsilon_4}{\epsilon_3}}\right), -\frac{1}{2}\left(\sqrt{\frac{\epsilon_2}{\epsilon_1}} + \sqrt{\frac{\epsilon_3}{\epsilon_4}}\right)\right) \quad (6)$$

for the rows of (5) combines elimination of all interior fluxes whenever possible with invariance under a rotation of 90° of the discretized equations for H_x and H_y. The resulting discretization for H_x at point P is

$$0 = \left(w\sqrt{\frac{\epsilon_2}{\epsilon_1}} + e\sqrt{\frac{\epsilon_3}{\epsilon_4}}\right)\frac{H_{xN} - H_{xP}}{2n} + \left(w\sqrt{\frac{\epsilon_1}{\epsilon_2}} + e\sqrt{\frac{\epsilon_4}{\epsilon_3}}\right)$$
$$\cdot \frac{H_{xS} - H_{xP}}{2s} + \left(n\sqrt{\frac{\epsilon_2}{\epsilon_1}} + n\sqrt{\frac{\epsilon_3}{\epsilon_4}} + s\sqrt{\frac{\epsilon_1}{\epsilon_2}} + s\sqrt{\frac{\epsilon_4}{\epsilon_3}}\right)$$
$$\cdot \frac{H_{xW} - H_{xP}}{4w} + \left(n\sqrt{\frac{\epsilon_2}{\epsilon_1}} + n\sqrt{\frac{\epsilon_3}{\epsilon_4}} + s\sqrt{\frac{\epsilon_1}{\epsilon_2}} + s\sqrt{\frac{\epsilon_4}{\epsilon_3}}\right)$$
$$\cdot \frac{H_{xE} - H_{xP}}{4e} + \frac{\omega^2\mu}{4}(n + s)$$
$$\cdot (w\sqrt{\epsilon_1\epsilon_2} + e\sqrt{\epsilon_3\epsilon_4})H_{xP} + \left(\sqrt{\frac{\epsilon_2}{\epsilon_1}} - \sqrt{\frac{\epsilon_1}{\epsilon_2}}\right)$$
$$\cdot \frac{H_{yW} - H_{yP}}{2}\left(\sqrt{\frac{\epsilon_4}{\epsilon_3}} - \sqrt{\frac{\epsilon_3}{\epsilon_4}}\right)\frac{H_{yE} - H_{yP}}{2}$$
$$- \frac{\beta^2}{4}\left(wn\sqrt{\frac{\epsilon_2}{\epsilon_1}} + ws\sqrt{\frac{\epsilon_1}{\epsilon_2}} + en\sqrt{\frac{\epsilon_3}{\epsilon_4}} + es\sqrt{\frac{\epsilon_4}{\epsilon_3}}\right)H_{xP}. \quad (7)$$

The equations, their coefficients, and the resulting discretized equation for H_y are obtained from those for H_x by rotating the labels in (5), (6), and (7) counterclockwise as follows:

$$x \mapsto y \mapsto -x$$
$$H_x \mapsto H_y \mapsto -H_x$$
$$n \mapsto w \mapsto s \mapsto e \mapsto n$$
$$N \mapsto W \mapsto S \mapsto E \mapsto N$$
$$1 \mapsto 2 \mapsto 3 \mapsto 4 \mapsto 1.$$

A formulation for smoothly varying dielectric permittivity $\epsilon(x, y)$ is given in [2]. The discretization in (7) can be used in this situation as well. To this end, ϵ_i should be taken to be $\epsilon(x, y)$ at the outside corner of the box Ω_i. With this interpretation of ϵ_i, our discretization for piecewise constant dielectric permittivity is consistent to first order with the equations for smoothly varying dielectric permittivity. The local truncation error of the discretization was evaluated by Taylor expansion of H_x, H_y, and ϵ, centered at the point P. This was done with the Maple system for symbolic computation [6].

This discretization yields a nonsymmetric generalized eigenvalue problem, $Kv = -\beta^2 Mv$. It can be seen from (7) that K has two diagonal blocks of five bands each for H_x and H_y, and two off-diagonal blocks of three bands each for the coupling terms, while M is a positive diagonal matrix. This generalized eigenvalue problem is recast as a standard eigenvalue problem, $Ax = -\beta^2 x$, where $A = M^{-1/2}KM^{-1/2}$ and $x = M^{1/2}v$.

III. Solution of the Eigenvalue Problem

For realistic grids, the use of standard dense matrix eigenvalue solvers leads to unmanageable CPU time and memory requirements, since the solution for all the possible eigenvalues is attempted. Only a small fraction of the eigenvalues correspond to confined modes. Because we wish to select these modes, we impose the condition

$$\mathrm{Re}\,(-\beta^2) < -\omega^2\mu\epsilon_{\mathrm{clad}}. \quad (8)$$

Here, ϵ_{clad} is the maximum value of the dielectric permittivity in the cladding region. The computational complex-

ity is greatly reduced by choosing an algorithm which computes this very limited subset of eigenpairs at the low end of the spectrum.

Appropriate algorithms for determining a subset of eigenvalues/eigenvectors of large, sparse, nonsymmetric matrices include simultaneous iteration [7], nonsymmetric Lanczos algorithm [8], and variations on the method of Arnoldi [9]. These are all projection methods [10]. We have chosen the method of Arnoldi as the basic algorithm for several reasons. First, Krylov subspace methods, such as the Lanczos and Arnoldi algorithms, have superior convergence properties for extremal eigenvalues [10] and can be effectively accelerated by preconditioning [11]. Also, numerical stability is improved by the modified Gram–Schmidt process in the Arnoldi iteration. Finally, the Arnoldi method can easily be generalized to find eigenvalues of any given multiplicity.

We have chosen to use Chebyshev polynomial preconditioning, which allows us to keep our matrix in banded storage, rather than resort to inverse iteration [12]. We precondition with the Chebyshev polynomial adapted to the reference ellipse through λ_r:

$$p_n(\lambda) = T_n\left(\frac{\lambda - d}{c}\right)\Big/ T_n\left(\frac{\lambda_r - d}{c}\right). \tag{9}$$

In our computations, we use a degenerate reference ellipse with $d - c = \lambda_r = -\omega^2 \mu \epsilon_{\text{clad}}$ and with $d + c$ an upper bound for the spectrum, as determined by Gerschgorin disks [13]. A typical example of p_n is plotted in Fig. 2. As n increases, $\| p_n(\lambda) \|$ approaches $[\kappa(\lambda)]^n$, where

$$\kappa(\lambda) = \frac{a(\lambda) + (a(\lambda)^2 - c^2)^{1/2}}{a(\lambda_r) + (a(\lambda_r)^2 - c^2)^{1/2}}$$

and $a(\lambda)$ is the major semiaxis of the ellipse through λ with center d and real foci $d - c$, $d + c$ [14], [15]. Thus, the strength of the preconditioning of λ depends on the distance between the confocal ellipses through λ and λ_r. The matrix-vector product $v_n = [p_n(A)]v_0$ is computed using the three-vector recursion [14], [15]

$$v_{i+1} = 2\frac{\sigma_{i+1}}{c}(A - dI)v_i - \sigma_i \sigma_{i+1} v_{i-1},$$

where

$$\sigma_{i+1} = \frac{1}{2/\sigma_1 - \sigma_i},$$

and $v_1 = (\sigma_1/c)(A - dI)v_0$, where $\sigma_1 = c/(\lambda_r - d)$. The three vectors $\{v_{i-1}, v_i, v_{i+1}\}$ are taken to be contiguous in the storage reserved for the next three Krylov vectors, thus reducing the need for access to slow memory—a typical bottleneck in supercomputing applications.

The Chebyshev—Arnoldi algorithm generates an orthonormal basis V_m for the Krylov subspace $K_m[p_n(A), v_0] = \text{span}\{v_0, [p_n(A)]v_0, [p_n(A)]^2 v_0, \cdots, [p_n(A)]^{m-1} v_0\}$. The Chebyshev polynomial preconditioning greatly magnifies the separation of the eigenvalues satisfying (8) relative to the rest of the spectrum, while leaving the eigenvectors unchanged. Convergence towards the desired eigenvectors is thus accelerated [12]. After finding the orthonormal basis V_m, we take a Rayleigh quotient $C_m = V_m^* A V_m$ of the operator A over the Krylov subspace. The spectral decomposition $C_m = Y_m \Lambda_m Y_m^{-1}$ is found using standard EISPACK routines. The approximate eigenvalues and eigenvectors of A are then Λ_m and $V_m Y_m$. The dominant one of these, and any others satisfying (8), are combined into a new starting vector v_0, and the whole process is repeated with stronger preconditioning, i.e., polynomials of higher degree n, until the residuals are within a prescribed tolerance. We have found this outer iteration to be effective in removing unwanted modes. Problems where double eigenvalues are expected because of symmetry must use two independent starting vectors v_0, w_0 and a double-vector Arnoldi method so that the projection subspace is $K_{m/2}[p_n(A), V_0] \oplus K_{m/2}[p_n(A), w_0]$. To obtain satisfactory convergence behavior in this case, one should also increase m.

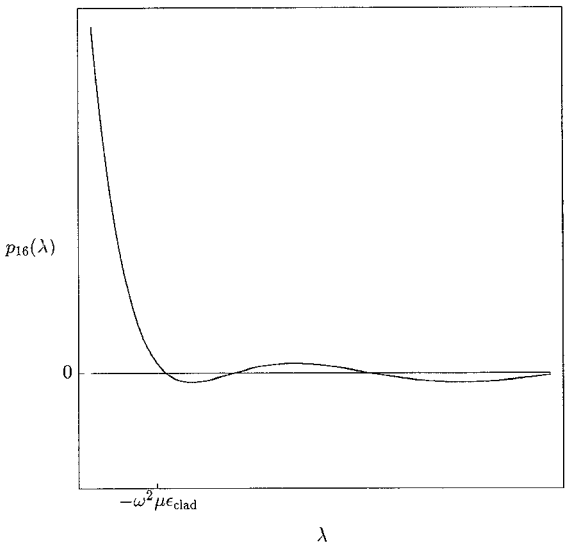

Fig. 2. The Chebyshev polynomial of (9) for $n = 16$.

Our algorithm is more effective for finding several eigenvectors than the Arnoldi–Chebyshev method [14], [15], which does not precondition the Arnoldi iteration, but only its starting vector. Chebyshev polynomial preconditioning allows difficult problems to be solved with a Krylov subspace of fixed size m. Limiting the size of the Krylov subspace also limits the computational complexity of the modified Gram–Schmidt orthogonalization in the Arnoldi algorithm. The storage requirement (in double precision real numbers) of the Chebyshev–Arnoldi algorithm itself is approximately $(2m + mblock + 3)N + 2m^2 + 3m$, where N is the total number of unknowns and $mblock$ is the maximum expected eigenvalue multiplicity. For our discretization, $N = 2(nx - 2)(ny - 2)$, where nx and ny are the number of grid lines in the x and y directions, and the banded matrix A requires storage of $8N$.

IV. Numerical Results

We present numerical results for a number of representative dielectric waveguides. The examples have been selected to facilitate comparison with previously published numerical approaches, as detailed below. For all computations we use a uniform grid in the core region. The mesh spacing grows exponentially as the lines extend far out into the cladding. Such grids both resolve rapid oscillations of higher modes in the core region and extend sufficiently far to allow the modes to decay exponentially into the cladding. The latter requirement is particularly relevant for modes close to their cutoff condition, as is the case in Fig. 6, which is discussed below. With two real field components at each grid point (and up to about a dozen complex unknowns per node in finite element discretizations of some similar problems [16]), such grids give rise to very large scale eigenvalue problems.

Our first example is a square waveguide. A double-vector Chebyshev–Arnoldi method with a Krylov subspace of dimension $m = 24$ was used. The dispersion plots in Fig. 3 generally agree with earlier results from [1], [17], [18]. For each mode, at low values of the normalized propagation constant B, we present results only for frequencies where there is sufficient decay within the discretized domain. Insisting on sufficient decay, we do not find the inflection points in the propagation curves for B near 0 that appear in [1]. It is likely that the inflection points in these propagation curves are due to the use of meshes with too few gridlines and over a spatial domain too small to allow natural decay of modes near cutoff.

The modes of the square waveguide reflect its invariance under a rotation of 90°. Double eigenvalues (dotted lines in Fig. 3) correspond to degenerate modes which are rotations of each other. Single eigenvalues (solid lines in Fig. 3) correspond to nondegenerate modes which are rotations of themselves. We could not label all modes unambiguously employing simple double integer indices. For example, because a lower mode should be labeled H^x_{21}, and a higher mode should be labeled H^x_{23}, the novel label $H^x_{2,1+2}$ was defined for the intermediate mode with H_x component shown in Fig. 4. In this labeling scheme, the additional indices correspond to "kinks" at interfaces, which are allowed by the interface matching conditions of (3) and (4). The size of these kinks decreases with increasing frequency ω, until a mode with kinks becomes indistinguishable from the corresponding mode without them. In other words, $A(\omega)$ becomes more nearly defective as $\omega \to \infty$.

Our second example is a channel waveguide. The dispersion plot is given in Fig. 5. A single-vector Chebyshev–Arnoldi method with a Krylov subspace of dimension $m = 20$ was used both for this example and the next one. There is good qualitative agreement with earlier results from [1], [17], [19]. Demonstrating the need for large computational grids, we show in Fig. 6 the H_x component of the H^x_{32} mode for the channel waveguide of Fig. 5 at a normalized frequency of $V = 2.10$, at which this

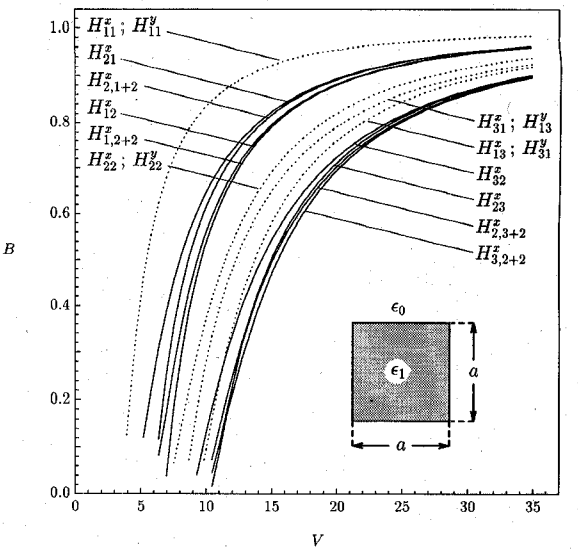

Fig. 3. Square waveguide. Normalized propagation constant $B = ((\beta/k_0)^2 - \epsilon_0)/(\epsilon_1 - \epsilon_0)$ versus normalized frequency $V = k_0 a(\epsilon_1 - \epsilon_0)^{1/2}$, with k_0 the free-space wavenumber. The computational domain is 5 μ × 5 μ, with $a = 1$ μ, $\epsilon_1 = 13.1\epsilon_0$. The discretization is on a 65 × 65 nonuniform rectangular grid. Solid lines indicate single modes and dotted lines double modes.

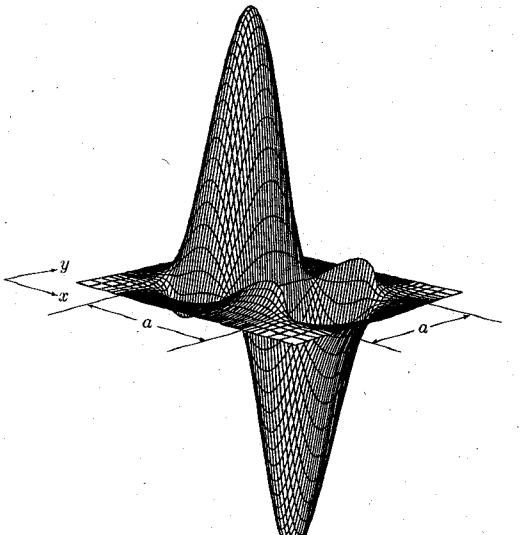

Fig. 4. $H^x_{2,1+2}$ mode (H_x component only) for a square waveguide as in Fig. 3 at a normalized frequency of $V = 11.0$. The plot is shown on a 55 × 55 centered subgrid.

mode has a normalized propagation constant of $B = .005$. For clarity, the plot is presented on a 55 × 33 subgrid in which it decays to 1% of its maximum over the total 69 × 38 domain. Such a large domain is necessary to properly capture the decay in the cladding region of any mode near cutoff.

The strip-slab waveguide is our third example. The dispersion plot of the H^y_{11} mode is shown in Fig. 7 for four different dielectric configurations as given in [1]. At low values of the normalized frequency V, the eigenfunctions expand considerably into the region of the cladding where the dielectric permittivity is highest. This effect is especially pronounced in case 4), where $\epsilon_4 = 2.575\epsilon_0$.

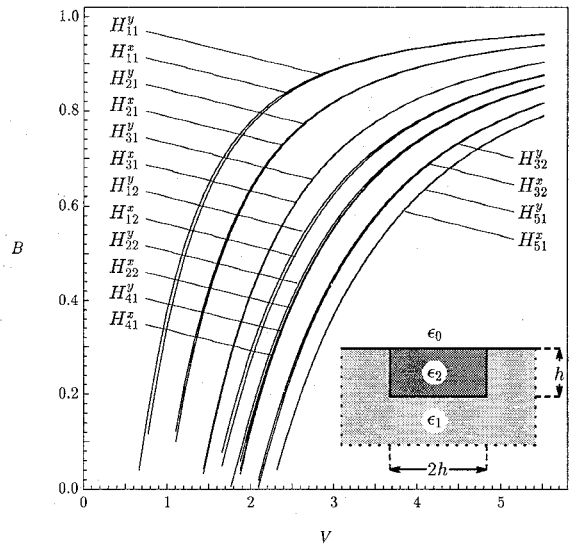

Fig. 5. Channel waveguide. Normalized propagation constant $B = ((\beta/k_0)^2 - \epsilon_1)/(\epsilon_2 - \epsilon_1)$ versus normalized frequency $V = (2h/\lambda)(\epsilon_2 - \epsilon_1)^{1/2}$, with k_0 the free-space wavenumber. The computational domain is 60 $\mu \times 32$ μ, with $h = 3$ μ, $\epsilon_1 = 2.13\epsilon_0$ and $\epsilon_2 = 2.25\epsilon_0$. The discretization is on a 69 $\times$ 38 nonuniform rectangular grid.

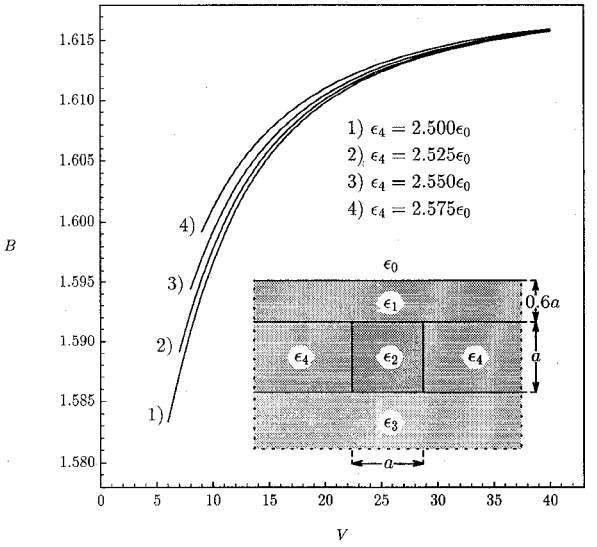

Fig. 7. Strip-slab waveguide. Normalized propagation constant $B = \beta/k_0$ versus normalized frequency $V = ak_0$, with k_0 the free-space wavenumber. The computational domain is 30 $\mu \times 30$ μ, with $a = 3$ μ, $\epsilon_1 = 2.55\epsilon_0$, $\epsilon_2 = 2.62\epsilon_0$, and $\epsilon_3 = 2.50\epsilon_0$. Dispersion plots for the fundamental mode H^y_{11} are shown, using four different values for ϵ_4. The discretization is on a 69 $\times$ 67 nonuniform rectangular grid.

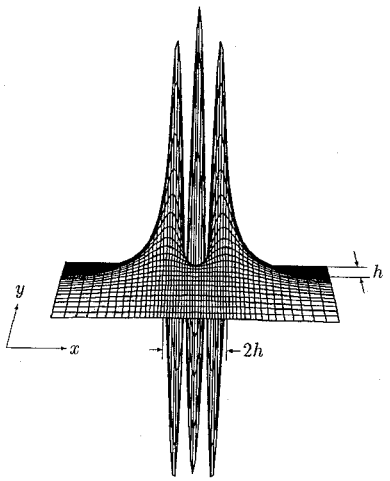

Fig. 6. H^x_{32} mode (H_x component only) for a channnel waveguide as in Fig. 5 at a normalized frequency of $V = 2.10$. The plot is shown on a 55 $\times$ 33 subgrid.

The computations were performed on a Sun 4/490 workstation. A typical execution time was aproximately 20 min to solve 16 modes in the square waveguide at a normalized frequency of $V = 13.9$, using the double-vector Chebyshev–Arnoldi method. For the channel waveguide, the execution times were considerably smaller, since a single-vector method was used. The solution for 16 modes at $V = 2.76$ was obtained in approximately 5 min.

V. Conclusion

Realistic modeling of dielectric waveguides requires solution of eigenvalue problems that are very large and sparse. The dense solvers used in [1], [2], [4], [16] find the complete spectral decomposition at the expense of greatly increased computational complexity and memory requirements, to the extent of prohibiting the solution on realistic grids. Since only the eigenvectors for the propagating modes are desired, projection methods are very suitable for these applications. The Chebyshev-preconditioned Arnoldi algorithm allowed us to simulate a wide range of problems employing variable meshes with large numbers of unknowns. The code we developed is robust and easy to use, with automatic selection of most parameters.

Acknowledgment

The authors are highly indebted to Professor A. Sameh who gave significant support over the course of this project in many useful discussions and who allowed us to use the facilities of the Center for Supercomputing Research and Development. We wish to thank R. Sanders for her help with the figures.

References

[1] K. Bierwirth, N. Schulz, and F. Arndt, "Finite-difference analysis of rectangular dielectric waveguide structures," *IEEE Trans. Microwave Theory Tech.*, vol. 34, no. 11, pp. 1104–1114, 1986.

[2] N. Schulz, K. Bierwirth, F. Arndt, and U. Köster, "Finite-difference method without spurious solutions for the hybrid-mode analysis of diffused channel waveguides," *IEEE Trans. Microwave Theory Tech.*, vol. 38, no. 6, pp. 722–729, 1990.

[3] R. Varga, *Matrix Iterative Analysis*. Prentice-Hall, Englewood Cliffs, NJ: 1962, p. 184.

[4] K. Hayata, M. Koshiba, M. Eguchi, and M. Suzuki, "Vectorial finite-element method without any spurious solutions for dielectric waveguiding problems using transverse magnetic-field component," *IEEE Trans. Microwave Theory Tech.*, vol. 34, no. 11, pp. 1120–1124, 1986.

[5] J. D. Jackson, *Classical Electrodynamics*, 2nd ed. New York: Wiley, 1974, pp. 17–22.

[6] B. W. Char, G. J. Fee, K. O. Geddes, G. H. Gonnet, and M. B.

Monagan, "A tutorial introduction to Maple," *J. Symbolic Computation*, vol. 2, no. 2, pp. 179–200, 1986.
[7] G. W. Stewart, "Simultaneous iteration for computing invariant subspaces of non-Hermitian matrices," *Numer. Math.*, vol. 25, pp. 123–136, 1976.
[8] B. N. Parlett, D. R. Taylor, and Z. A. Liu, "A look-ahead Lanczos algorithm for unsymmetric matrices," *Math. Comp.*, vol. 44, pp. 105–124, 1985.
[9] Y. Saad, "Variations of Arnoldi's method for computing eigenelements of large unsymmetric matrices," *Linear Algebra and Its Applications*, vol. 34, pp. 269–295, 1980.
[10] ——, "Projection methods for solving large sparse eigenvalue problems," in *Matrix Pencils, Proceedings*, vol. 973 of *Lecture Notes in Math.*, pp. 121–144, Springer-Verlag, 1982.
[11] V. I. Agoshkov, and J. A. Kuznetsov, "Lanczos method for the eigenvalue problem," in *Comp. Meth. Linear Algebra*, G. I. Marchuk, Ed., pp. 145–164, 1972 (in Russian).
[12] R. Natarajan, "An Arnoldi-based iterative scheme for nonsymmetric matrix pencils arising in finite element stability problems," Tech. Rep. RC 16327 (#69303), IBM Thomas J. Watson Research Center, Yorktown Heights, NY, 1990.
[13] G. H. Golub and C. F. Van Loan, *Matrix Computations*, 2nd ed. Baltimore, MD: Johns Hopkins University Press, 1989.
[14] Y. Saad, "Chebyshev acceleration techniques for solving nonsymmetric eigenvalue problems," *Math. Comp.*, vol. 42, no. 166, pp. 567–588, 1984.
[15] D. Ho, F. Chatelin, and M. Bennani, "Arnoldi–Tchebychev procedure for large scale nonsymmetric matrices," *Math. Model. Numer. Anal.*, vol. 24, no. 1, pp. 53–65, 1990.
[16] J. Svedin, "A modified finite-element method for dielectric waveguides using an asymptotically correct approximation on infinite elements," *IEEE Trans. Microwave Theory Tech.*, vol. 39, no. 2, pp. 258–266, 1991.
[17] E. A. J. Marcatili, "Dielectric rectangluar waveguide and directional coupler for integrated optics," *Bell Syst. Tech. J.*, vol. 48, pp. 2071–2102, 1969.
[18] E. Schweig and W. B. Bridges, "Computer analysis of dielectric waveguides: A finite-difference method," *IEEE Trans. Microwave Theory Tech.*, vol. 32, no. 5, pp. 531–541, 1984.
[19] B. M. A. Rahman and J. B. Davis, "Penalty function improvement of waveguide solution by finite elements," *IEEE Trans. Microwave Theory Tech.*, vol. 32, pp. 922–928, 1984.

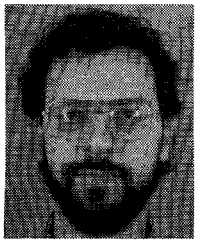

Albert T. Galick was born in New Brunswick, NJ, on July 23, 1958. He received the B.S. degree in mathematics in 1980 from the Massachusetts Institute of Technology, Cambridge, and the M.S. degree in mathematics in 1984 from the University of Illinois at Urbana-Champaign (UIUC).

He worked at AT&T as a COBOL programmer in 1980 and as a C programmer from 1984 to 1986. Since 1986, he has been a Research Assistant at UIUC's Center for Supercomputing Research and Development, while working toward the Ph.D. degree in computer science. His thesis treats large, sparse eigenvalue problems, specifically those arising in numerical simulations of electronic and electromagnetic devices.

Thomas Kerkhoven received the Drs. degree in Physics from the University of Amsterdam in 1981, and the Ph.D. in numerical analysis from the Department of Computer Science at Yale University in 1985. Since 1986 he has been at the University of Illinois in Urbana-Champaign, originally as Assistant Professor, and since 1989 as Associate Professor. In 1990, he spent a semester as consultant at AT&T Bell Laboratories, Murray Hill, NJ and in 1991 a semester as visiting Associate Professor at Duke University.

His research focuses on the development of numerical techniques for the design of microelectronic devices. At the University of Illinois his primary appointment is with the department of Computer Science. Moreover, he holds appointments with the department of Electrical and Computer Engineering, and the Beckman Institute of Advanced Science and Technology at the University of Illinois.

Umberto Ravaioli (M'88) was born in 1955 in Forli, Italy. He received the Laurea Dr. in electronics engineering and the Laurea Dr. in Physics from the University of Bologna, Italy, in 1980 and 1982, respectively, and the Ph.D. in electrical engineering from Arizona State University in 1986.

In 1982 he was a Research Fellow of the U. Bordoni Foundation, Rome, for studies on microwave circuits and propagation. He joined the Department of Electrical and Computer Engineering of the University of Illinois at Urbana-Champaign in 1986, where he is now an Associate Professor. Dr. Ravaioli's current research mainly focuses on the physics and the numerical simulation of high speed semiconductor devices, including aspects of supercomputation and visualization. His main interests are in the areas of Monte Carlo particle simulation, energy balance modeling, optoelectronic and quantum devices.